

Conquer the fine structure splitting of excitons in self-assembled InAs/GaAs quantum dots via combined stresses

Jianping Wang,¹ Ming Gong,² Guang-Can Guo,¹ and Lixin He^{1, a)}

¹⁾Key Laboratory of Quantum Information, University of Science and Technology of China, Hefei, Anhui, 230026, People's Republic of China

²⁾Department of Physics and Astronomy, Washington State University, Pullman, Washington, 99164 USA

(Dated: 29 August 2021)

Eliminating the fine structure splitting (FSS) of excitons in self-assembled quantum dots (QDs) is essential to the generation of high quality entangled photon pairs. It has been shown that the FSS has a lower bound under uniaxial stress. In this letter, we show that the FSS of excitons in a general self-assembled InGaAs/GaAs QD can be fully suppressed via combined stresses along the [110] and [010] directions. The result is confirmed by atomic empirical pseudopotential calculations. For all the QDs we studied, the FSS can be tuned to be vanishingly small ($< 0.1 \mu\text{eV}$), which is sufficient small for high quality entangled photon emission.

There has been continuous interest in finding an efficient entangled photon source for quantum information applications. Benson *et al.* proposed that a biexciton cascade process in a self-assembled quantum dot (QD) can be used to generate the “event-ready” entangled photon pairs.¹ In this scheme, a biexciton decays into two photons via two paths of different polarizations $|H\rangle$ and $|V\rangle$. If the two paths are indistinguishable, the two emitted photons are polarization entangled.^{1,2} Unfortunately, the $|H\rangle$ - and $|V\rangle$ -polarized photons may have a small energy difference, known as the fine structure splitting (FSS),^{3,4} due to the asymmetric electron-hole exchange interaction in the QDs.^{5,6} The FSS is typically about $-40 \sim +80 \mu\text{eV}$ in the InAs/GaAs QDs,⁷ which is much larger than the radiative linewidth ($\sim 1.0 \mu\text{eV}$), and therefore provides “which way” information about the photon decay path that destroys the photon entanglement.^{2,8} Although, it is possible to “cherry-pick” a QD that has tiny FSS from a large amount of QDs,² it is highly desired that the FSS can be tuned by the external fields in a controlled way. Indeed, it has been successfully demonstrated that the FSS can be tuned by electric fields,^{9–13} magnetic fields,¹⁴ and uniaxial stress.^{15,16}

Applying a stress is an effective way to reduce the FSS in a QD experimentally.^{15,16} For an ideal QD with C_{2v} symmetry, the FSS can be reduced to exact zero when the stress is applied along the [110] direction.¹⁷ However, for a general QD with C_1 symmetry, there is a lower bound for the FSS¹⁷ because the two bright states belong to the same symmetry representation. Gong *et al.*¹⁸ derived a general relation between the FSS, the exciton polarization angle and the uniaxial stress. They have shown that the FSS lower bound can be predicted by the polarization angle and the FSS under zero stress. Similar relationship is also found when the FSS is tuned by vertical electric field,¹³ where the minimal FSS under electric field can be as small as $0.7 \mu\text{eV}$. However, for most of

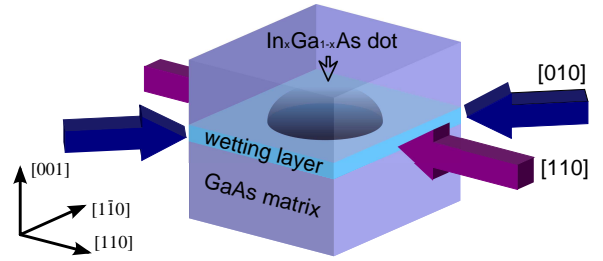


FIG. 1. The InGaAs QD is embedded in a $60 \times 60 \times 60$ GaAs matrix. External stresses are applied along the [010] and [110] directions simultaneously.

the dots, the minimal FSS under vertical electric field is still larger than the required splitting to observe entangled photons emission (see Supplementary Information in Ref. 13, where 16 of the 22 studied dots have the minimum FSS above $2.5 \mu\text{eV}$). One may ask whether we can further reduce the FSS of a *general* QD by the external electric fields or stresses, to nearly zero.

In this Letter, we demonstrate that indeed the FSS of a general self-assembled InGaAs/GaAs QDs with C_1 symmetry can be tuned to be vanishingly small by applying combined stresses along the [110] and [010] directions. The results are confirmed by atomistic empirical pseudopotential calculations.^{19,20} The minimal FSS is generally below $0.1 \mu\text{eV}$, which is sufficient for high quality on-demand entangled photon emissions.

In a previous work, Gong *et al.* proposed an exciton Hamiltonian under uniaxial stress,¹⁸

$$H(\mathbf{n}, p) = H_{2v} + V_1 + V_s(\mathbf{n})p, \quad (1)$$

where \mathbf{n} is the external stress direction, and p is the magnitude of the stress. H_{2v} represent the Hamiltonian of an ideal QD with C_{2v} symmetry, whereas V_1 lower the dot symmetry to C_1 , due to local structure deformations, alloy distribution²¹ and interfacial effects²² etc. $V_s(\mathbf{n})p$ is the potential change due to the external stress. Note that the lattice deformation under external stress ($< 10^2$ MPa) is generally smaller than 0.1%, thus in the above

^{a)}Electronic mail: helx@ustc.edu.cn

Hamiltonian the term $O(p^2)$ is omitted. The eigenvectors of the two bright states of H_{2v} are $|3\rangle = |\Gamma_2\rangle + i|\Gamma_4\rangle$ and $|4\rangle = |\Gamma_2\rangle - i|\Gamma_4\rangle$, with corresponding eigenvalues E_3 and E_4 , respectively. In the absence of an in-plane magnetic field, the coupling between the dark states and bright states is negligible. We therefore write the Hamiltonian in the space spanned by the two bright states of H_{2v} ,

$$H = \begin{pmatrix} \bar{E} + \delta + \alpha_3 p & \kappa + \beta p \\ \kappa + \beta p & \bar{E} - \delta + \alpha_4 p \end{pmatrix}, \quad (2)$$

where $\bar{E} + \delta = \langle 3|H_{2v} + V_1|3\rangle$, $\bar{E} - \delta = \langle 4|H_{2v} + V_1|4\rangle$. $\alpha_i = \langle i|V_s(\mathbf{n})|i\rangle$ ($i=3, 4$), $\kappa = \langle 3|V_1|4\rangle$ and $\beta = \langle 3|V_s(\mathbf{n})|4\rangle$. Because the Hamiltonian has a time-reversal symmetry, all parameters can therefore be set to real values for simplicity. We define $\alpha = \alpha_3 - \alpha_4$ and $\gamma = \alpha_3 + \alpha_4$. The eigenstates of the two bright states are the linear combination of states, $|3\rangle$, $|4\rangle$ i.e., $|\psi_-\rangle = \cos\theta|3\rangle + \sin\theta|4\rangle$ and $|\psi_+\rangle = -\sin\theta|3\rangle + \cos\theta|4\rangle$. The FSS $\Delta(p)$ for QDs under uniaxial stress p is,

$$\Delta(p) = \sqrt{4(\beta p + \kappa)^2 + (\alpha p + 2\delta)^2}. \quad (3)$$

According to the symmetry analysis (and verified by the atomistic theory), one has $\beta = 0$ when the stress is applied along the $[110]$ ($[\bar{1}\bar{1}0]$) direction, and $\alpha=0$, if the stress is applied along the $[010]$ ($[100]$) direction.¹⁸ Since the uniaxial stress can not make $(\beta p + \kappa)$ and $(\alpha p + 2\delta)$ equal to zero simultaneously, there is always a lower bound for FSS when $\kappa\delta \neq 0$, which is determined by $2|\kappa|$ or $2|\delta|$ depending on the direction of the stress.

The above results suggest that diagonal and off-diagonal terms of the Hamiltonian matrix Eq. (2) can be tuned by the stress along the $[110]$ and $[010]$ directions independently. Therefore, it is possible to further reduce the FSS by applying the stresses along the $[110]$ and $[010]$ directions simultaneously. To show this, we generalize the 2×2 model exciton Hamiltonian under uniaxial stress to that under the combined stresses,

$$H = \begin{pmatrix} \bar{E} + \delta + \alpha_3 p_{[110]} & \kappa + \beta p_{[010]} \\ \kappa + \beta p_{[010]} & \bar{E} - \delta + \alpha_4 p_{[110]} \end{pmatrix}. \quad (4)$$

The FSS for QDs under the combined stress is

$$\Delta(p) = \sqrt{4(\beta p_{[010]} + \kappa)^2 + (\alpha p_{[110]} + 2\delta)^2}. \quad (5)$$

The polarization angle θ vs $p_{[110]}$ and $p_{[010]}$ can be calculated from,

$$\tan(\theta_{\pm}) = \frac{-2\delta - \alpha p_{[110]} \mp \Delta(p)}{2(\beta p_{[010]} + \kappa)} \quad (6)$$

Naively, one may expect that by choosing $p_{[010]} = -\kappa/\beta$ and $p_{[110]} = -2\delta/\alpha$, the FSS can be tuned to be exactly zero. However, it should be noted that the exact zero FSS is forbidden by the symmetry restriction for a QD with C_1 symmetry. In the above model, we neglect the

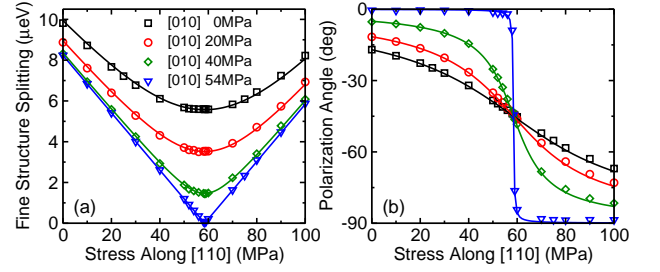


FIG. 2. Change of FSS (a) and polarization angle (b) under the combined stress along the $[110]$ and $[010]$ directions for the lens-shaped $\text{In}_{0.6}\text{Ga}_{0.4}\text{As}/\text{GaAs}$ dot. The scatters are the results of numerical calculations whereas the solid lines are the results of the two-level model.

higher order terms, which may become important when FSS becomes very small. To see what is the minimal FSS one can obtain under the combined stresses, we perform atomistic empirical pseudopotential calculations^{19,20} on the FSS under the combined stress along the $[010]$ and $[110]$ directions. Remarkably, we find that the FSS of a general $\text{InGaAs}/\text{GaAs}$ QD can be reduced to be vanishingly small ($<0.1 \mu\text{eV}$) under the combined stresses.

The $\text{InGaAs}/\text{GaAs}$ QDs are modeled by embedding the InGaAs dots in a $60 \times 60 \times 60$ 8-atom GaAs supercell. The QDs are assumed to be grown along the $[001]$ direction, on top of the one monolayer InAs wetting layers. We apply combined stresses along the $[110]$ and the $[010]$ directions as shown in Fig. 1. The stresses can be either compressive or tensile depending on the structure of QDs. The resultant deformation of the supercell under stresses is approximated by the linear superposition of the deformation of the cell under individual uniaxial stresses. Optimal atomic positions under stresses are obtained with valence force field method.^{23,24} We solve the Schrödinger equation to obtain the single-particle energy levels and wavefunctions using a strained linear combination of Bloch band method.²⁵ The exciton energies are then calculated via the many-particle configuration interaction method,²⁶ in which the exciton wave functions are expanded in Slater determinants constructed from all confined electron and hole single-particle states.

We have calculated 8 InAs/GaAs QDs with different geometries, including (elongated-)lens, pyramid, truncated cone, etc. and different alloy compositions. Here we take a lens-shaped $\text{In}_x\text{Ga}_{1-x}\text{As}/\text{GaAs}$ dot with $x = 0.6$, diameter $D = 25$ nm, and height $h = 3.5$ as an example. We obtain similar results for all other QDs. Fig. 2 depicts the behavior of the FSS and polarization angle of the dot under combined $[110]$ and $[010]$ stresses. We plot the FSS and exciton polarization angles as functions of stress along the $[110]$ direction under $p_{[010]} = 0, 20, 40$ and 54 MPa. For a given stress along the $[010]$ direction, the FSS goes through an anti-crossing as a function of stress along the $[110]$ direction, which is very similar to the results under uniaxial stress.¹⁸ The critical stress along the $[110]$ direction changes little with the stress applied along

TABLE I. Parameters for $\text{In}_x\text{Ga}_{1-x}\text{As}/\text{GaAs}$ QDs with different shape and compositions under combined stresses along the [110] and [010] directions. The unit of dot diameter D and height h is nm. The fine structure $\Delta(p)$ is in unit of μeV and the combined critical stresses $p_c = (p_{[110]}, p_{[010]})$ are in unit of MPa.

QDs	Pesudopotential Calculation		Model Parameters and Predictions				
	$\Delta(p_c)$	p_c	α	δ	β	κ	p_c
Cone ($x = 0.6$) $D = 25, h = 3.5$	0.084	(58.0, -36.0)	-0.15	4.36	0.06	2.04	(58.6, -36.1)
Truncated Cone ($x = 0.6$) $D_B = 25$ $D_T = 20, h = 3.5$	0.032	(11.3, -45.7)	-0.14	0.79	0.05	2.23	(11.5, -46.0)
Elongated Lens ($x = 0.6$) $D_{[110]} = 20$ $D_{[1\bar{1}0]} = 25, h = 3.5$	0.045	(75.8, -19.8)	-0.17	6.37	0.06	1.24	(76.0, -20.1)
Elongated Lens ($x = 0.6$) $D_{[110]} = 25$ $D_{[1\bar{1}0]} = 20, h = 3.5$	0.076	(-36.8, -10.7)	-0.17	3.03	0.06	0.70	(-36.6, -11.4)
Lens ($x = 0.8$) $D = 25, h = 3.5$	0.048	(35.6, 14.0)	-0.19	3.46	0.06	-0.89	(35.8, 14.1)
Lens ($x = 0.6$) $D = 25, h = 3.5$	0.039	(58.5, 54.0)	-0.14	4.11	0.05	-2.79	(58.5, 54.3)
Lens ($x = 0.6$) $D = 25, h = 5.0$	0.083	(-12.4, -43.6)	-0.13	-0.79	0.045	1.99	(-12.2, -43.8)
Pyramid ($x = 0.6$) $D = 25, h = 3.5$	0.075	(27.5, 1.6)	-0.13	1.77	0.051	-0.092	(28.0, 1.78)

the [010] direction. However the minimal FSS changes dramatically for different stresses applied along the [010] direction, as we expected. When no stress is applied, the FSS of the QD is approximately $9.8 \mu\text{eV}$. When we apply the stress along the [110] direction, one can reduce the FSS to approximately $5.6 \mu\text{eV}$, and $8.2 \mu\text{eV}$ if the stress is applied along the [010] direction. In either case, the FSS is much larger than $1 \mu\text{eV}$ to suitable for high quality entangled photon emitters. However, when combined stresses along the [110] and [010] directions are applied, the lowest FSS we obtain is $0.04 \mu\text{eV}$ at $p_{[110]}=58.5$ MPa and $p_{[010]}=54$ MPa. The polarization angles rotate clockwise or anticlockwise depending on the magnitude of stress along the [010] direction and the polarization angle at the critical stress always tends to be -45° or 45° . The calculated FSS and exciton polarization angles are in excellent agreement with model predictions. The minimal FSS of all other QDs are also $<0.1 \mu\text{eV}$ under the combined stresses (See Table I for critical stresses and the FSS minimum of all dots we studied). The tunable area in which FSS is less than $1 \mu\text{eV}$ is proportional to $2/|\alpha|$ and $1/|\beta|$. In typical $\text{InGaAs}/\text{GaAs}$ dots, $|\alpha| \sim 0.1\text{-}0.4 \mu\text{eV}/\text{MPa}$ and $|\beta| \sim 0.04\text{-}0.1 \mu\text{eV}/\text{MPa}$,¹⁸ therefore the tunable area for FSS less than $1 \mu\text{eV}$ is approximately $5 \times 10 \text{ MPa}^2$, which is easy to control in experiments.

When the stresses along the two directions approach the critical point at the same time, the FSS becomes very small, the higher order terms in Eq. (4) may not be ignored, and therefore the FSS can never be exactly zero. Such higher order terms are fully included in the atomistic calculation. The comparison between the model predictions and exact numerical simulations can reveal the role of these terms. As shown in Fig. 2, the numerical

results (scatters) and two-level model predictions (solid lines), using the parameters fitted from the results of uniaxial stress, are in excellent agreement. This suggests that the higher order terms are indeed unimportant except extremely close to the critical stresses.

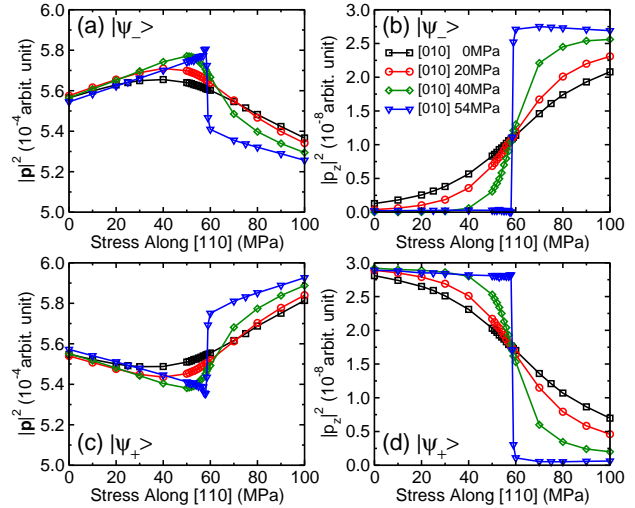


FIG. 3. Left panel: The change of the total dipole moment under the stresses for the two bright states: $|\psi_- \rangle$ (a) and $|\psi_+ \rangle$ (c), in the lens-shaped $\text{In}_{0.6}\text{Ga}_{0.4}\text{As}/\text{GaAs}$ dot. Right panel: The change of the z -component of dipole moment under combined stresses for the two bright states: $|\psi_- \rangle$ (b) and $|\psi_+ \rangle$ (d).

Figure 3(a), 3(c) depict the total dipole moment $|\mathbf{p}|^2 = p_x^2 + p_y^2 + p_z^2$ of the two bright states under combined stresses. The total dipole moments of the two

states change a little in opposite directions under the stresses, and the lifetimes of the excitons change accordingly. However, the sum of the total dipole moments of the two bright states shows very little change ($< 1\%$) for stresses up to 100 MPa. Interestingly, for applied stress $p_{[010]} = 54$ MPa (critical stress along the $[010]$ direction), the total dipole moments of the two states change suddenly near the critical stress $p_{[110]} = 58$ Mpa. This is because, at $p_{[010]} = 54$ MPa, the dipole moments of the two states are approximately aligned along the $[110]$ and $[\bar{1}\bar{1}0]$ directions, with one increases whereas one decreases under the stress along the $[110]$ direction. When the stress approach the critical stress along the $[110]$ direction, the polarization angle rotates very fast from 0° to -90° , i.e., the two states switch polarization, which causes the jump of the total dipole moments of the two states. There are also very small z components of the dipole moment p_z because of the valence band mixing, as shown in Fig. 3(b), 3(d). Therefore, when we project the dipole moment into the x-y plane, the polarization of the two bright states are not exactly orthogonal to each other. The deviation is approximately $1^\circ - 2^\circ$.

Bennett *et al.* have successfully tuned the FSS by applying a vertical electric field.¹³ According to the symmetry analysis, the effect of a vertical electric field is equivalent to the uniaxial stress along the $[110]$ direction. Therefore, it is also possible to tune the FSS to approximately zero by applying a combined vertical electric field and an uniaxial stress along the $[010]$ direction, which might be more feasible experimentally. We leave this for future study.

To summarize, we have demonstrated that the FSS in general self-assembled QDs can be reduced to nearly zero under combined stresses along the $[110]$ and $[010]$ directions. A wide range of stresses can reduce the FSS to less than $1 \mu\text{eV}$ and thus provide great merit in experiments.

LH acknowledges the support from the Chinese National Fundamental Research Program 2011CB921200, National Natural Science Funds for Distinguished Young Scholars, and the Fundamental Research Funds for the Central Universities No. WK2470000006.

¹O. Benson, C. Santori, M. Pelton, and Y. Yamamoto, Phys. Rev. Lett. **84**, 2513 (2000).

²R. M. Stevenson, R. J. Young, P. Atkinson, K. Cooper, D. A. Ritchie, and A. J. Shields, Nature **439**, 179 (2006).

- ³D. Gammon, E. Snow, B. Shanabrook, D. Katzer, and D. Park, Phys. Rev. Lett. **76**, 3005 (1996).
- ⁴M. Bayer, G. Ortner, O. Stern, A. Kuther, A. A. Gorbunov, A. Forchel, P. Hawrylak, S. Fafard, K. Hinzer, T. L. Reinecke, S. N. Walck, J. P. Reithmaier, F. Klopff, and F. Schäfer, Phys. Rev. B **65**, 195315 (2002).
- ⁵G. Bester, S. Nair, and A. Zunger, Phys. Rev. B **67**, 161306 (2003).
- ⁶L. He, M. Gong, C.-F. Li, G.-C. Guo, and A. Zunger, Phys. Rev. Lett. **101**, 157405 (2008).
- ⁷R. J. Young, R. M. Stevenson, A. J. Shields, P. Atkinson, K. Cooper, D. A. Ritchie, K. M. Groom, A. I. Tartakovskii, and M. S. Skolnick, Phys. Rev. B **72**, 113305 (2005).
- ⁸R. Hafenbrak, S. Ulrich, P. Michler, L. Wang, A. Rastelli, and O. Schmidt, New J. of Phys. **9**, 315 (2007).
- ⁹K. Kowalik, O. Krebs, A. Lemaitre, S. Laurent, P. Senellart, P. Voisin, and J. Gaj, Appl. Phys. Lett. **86**, 041907 (2005).
- ¹⁰B. D. Gerardot, S. Seidl, P. A. Dalgarno, R. J. Warburton, D. Granados, J. M. Garcia, K. Kowalik, O. Krebs, K. Karrai, A. Badolato, and P. M. Petroff, Appl. Phys. Lett. **90**, 041101 (2007).
- ¹¹M. Vogel, S. Ulrich, R. Hafenbrak, P. Michler, L. Wang, A. Rastelli, and O. Schmidt, Appl. Phys. Lett. **91**, 051904 (2007).
- ¹²S. Marcet, K. Ohtani, and H. Ohno, Appl. Phys. Lett. **96**, 101117 (2010).
- ¹³A. J. Bennett, M. A. Pooley, R. M. Stevenson, M. B. Ward, R. B. Patel, A. B. de la Giroday, N. Sköld, I. Farrer, C. A. Nicoll, D. A. Ritchie, and A. J. Shields, Nature Phys. **6**, 947 (2010).
- ¹⁴R. M. Stevenson, R. J. Young, P. See, D. G. Gevanx, K. Cooper, P. Atkinson, I. Farrer, D. A. Ritchie, and A. J. Shields, Phys. Rev. B **73**, 033306 (2006).
- ¹⁵S. Seidl, M. Kroner, A. Högele, K. Karrai, R. J. Warburton, A. Badolato, and P. M. Petroff, Appl. Phys. Lett. **88**, 203113 (2006).
- ¹⁶J. D. Plumhof, V. Krápek, F. Ding, K. D. Jöns, R. Hafenbrak, P. Klenovský, A. Herklotz, K. Dörr, P. Michler, A. Rastelli, and O. G. Schmidt, Phys. Rev. B **83**, 121302 (2011).
- ¹⁷R. Singh and G. Bester, Phys. Rev. Lett. **104**, 196803 (2010).
- ¹⁸M. Gong, W. Zhang, G.-C. Guo, and L. He, Phys. Rev. Lett. **106**, 227401 (2011).
- ¹⁹A. J. Williamson, L.-W. Wang, and A. Zunger, Phys. Rev. B **62**, 12963 (2000).
- ²⁰G. Bester, J. Phys.: Condens. Matter **21**, 23202 (2009).
- ²¹V. Mlinar and A. Zunger, Phys. Rev. B **79**, 115416 (2009).
- ²²G. Bester and A. Zunger, Phys. Rev. B **71**, 045318 (2005).
- ²³P. N. Keating, Phys. Rev. **145**, 637 (1966).
- ²⁴R. Martin, Phys. Rev. B **1**, 4005 (1970).
- ²⁵L.-W. Wang and A. Zunger, Phys. Rev. B **59**, 15806 (1999).
- ²⁶A. Franceschetti, H. Fu, L.-W. Wang, and A. Zunger, Phys. Rev. B **60**, 1819 (1999).